ELSEVIER

Journal of Chromatography A, 680 (1994) 109–116

JOURNAL OF CHROMATOGRAPHY A

Extended path length post-column flow cell for UV–visible absorbance detection in capillary electrophoresis

Suhyeon Kim, Weonseop Kim, Jong Hoon Hahn*

Center for Biofunctional Molecules, Department of Chemistry, Pohang University of Science and Technology, San 31 Hyoja Dong, Pohang 790–784, South Korea

Abstract

A new type of post-column flow cell with extended optical path length has been developed to improve sensitivity of UV–visible absorbance detection for capillary electrophoresis. In this flow cell, the outlet of the capillary column is connected vertically to the middle of a 3-mm microchannel. Auxiliary flows are employed to flush substances eluted from the outlets of the microchannel. The optical path length is the full length of the microchannel. An 8-fold signal-to-noise ratio improvement over on-column detection has been demonstrated. However, the post-column flow cell suffered 44% loss in resolution. A limit of detection of $3.2 \cdot 10^{-7}$ M has been obtained for fluorescein isothiocyanate.

1. Introduction

Capillary electrophoresis (CE) is an elegant separation technique for the analysis of a wide variety of complex mixtures [1–6]. Typically, CE uses fused-silica capillary columns with inner diameters of 25–100 μm. The narrow diameter columns provide CE with several advantages such as short analysis times, remarkably high separation efficiency, and minimal sample volume requirements. However, in the case of conventional on-column UV–visible absorbance detection, the short optical path length available in such small capillaries limits the detection sensitivity and typically results in limits of detection (LOD) of 10^{-5}–10^{-6} M.

Recently, several interesting methods have been employed to increase the path length for UV–visible absorbance detection in CE [7–12]. Tsuda et al. [9] investigated the use of transparent rectangular borosilicate glass capillaries as an alternative to cylindrical capillaries. Dimensions of the rectangular capillaries ranged from 16 μm × 195 μm to 50 μm × 1000 μm. Detection across the long cross-sectional axis provided up to 15-fold increase in sensitivity. Xi and Yeung [10] devised a means of axially illuminating the full length of the capillary, and obtained a 7-fold increase in sensitivity for a 50-μm I.D. capillary and 3-mm injection plugs. Chervet et al. [11] extended the short optical path lengths in microcapillaries by bending the capillary into a Z shape and illuminating through the bend. A 6-fold improvement in signal-to-noise ratio (S/N) has been demonstrated with Z-shaped flow cells where light is transmitted through a 3-mm bend. The sensitivity of the Z-shaped flow cells has been greatly enhanced by optimizing light throughput in a 3-mm capillary section using a quartz ball lens [12].

* Corresponding author.

0021-9673/94/$07.00
SSDI 0021-9673(94)00679-2

Moring et al. [8] analyzed ray traces of light in the capillary bend of Z-shaped flow cells. This work has shown that the curved structure of the Z-cells requires focusing incident light with a special optics such as a quartz ball lens and offsetting the lens from capillary axis to maximize the light path length and the total light transmission through a bend. Moreover, the maximum effective path length for light transmitted through the bend was found to be much shorter than the length of the optical segment of a Z-cell. For example, the effective path length for a 75-μm capillary with outer diameter of 280 μm was at best 1.33 mm corresponding to 44% of the length of the optical segment (3 mm) of the cell. Therefore, avoiding any bent parts along the capillary's longitudinal axis in the optical segment of flow cells with extended optical path length is a logical extention of the Z-shaped cells for enhancing further the sensitivity of UV–visible absorbance detection in CE.

In this paper, we propose a new method of increasing path length for UV–visible absorbance detection in CE. Fig. 1 schematically shows the proposed extended path length flow cell with a post-column configuration. At the outlet of the capillary column, the eluted solution is splitted into two flows that travel in opposite directions through the microchannel

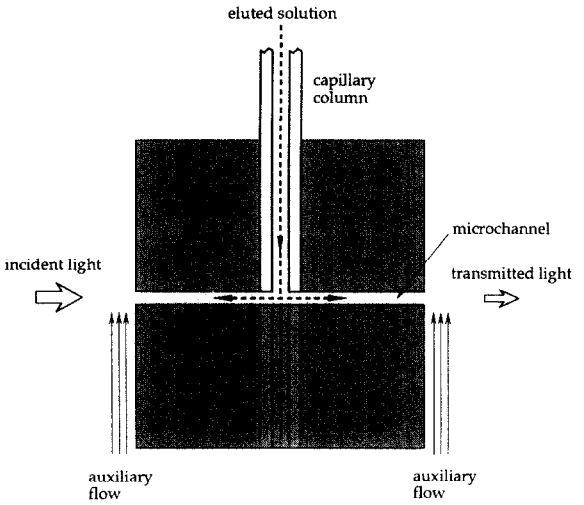

Fig. 1. Schematic of the post-column microchannel flow cell.

positioned vertically to the column. The microchannel is connected to the column outlet at the middle of the channel. Accumulation of eluted substances at both outlets of the channel is prevented by continuously flushing the outlets with a buffer solution. The optical segment of the proposed flow cell is the straight microchannel. Illuminating the microchannel with light collimated to the direction of the longitudinal axis of the channel allows us to utilize the full length of the channel as the optical path length.

In addition to the extended optical path length, our post-column microchannel flow cells enjoy several other potential advantages for optical detection in CE. First, in the case of extended path length on-column flow cells, such as Z-shaped ones [11,12], the bent configuration requires special optical couplings to optimize light throughput [12]. However, the unbent configuration of the post-column flow cells can make the optical coupling easier. Secondly, if the proposed post-column flow cells are provided with an additional influent branch channel for a derivatizing reagent around the outlet of the capillary column, post-column derivatization and sensitive detection can be accomplished at the same time. Finally, because actual shapes and materials of the flow cells can be changed, while keeping essential features for the extended path length post-column detection, the flow cells can be adopted to nearly all kinds of coherent or incoherent optical detection techniques (e.g., absorption, fluorescence and thermo-optical absorption). The purpose of this paper is to demonstrate the feasibility of the extended path length post-column flow cells for UV–visible absorbance detection in CE.

2. Experimental

2.1. Reagents

All chemicals were of analytical-reagent grade and used without further purification. Deionized water was prepared with a Mega-Pure system (Barnstead, Dubuque, IA, USA). Dansyl-amino acids, fluorescein isothiocyanate (FITC) and all

inorganic chemicals were purchased from Sigma (St. Louis, MO, USA). Buffer solutions were filtered through 0.2-μm membrane filters (cellulose nitrate; Whatman, Maidstone, UK) and degassed by sonication for 5 min just before using. Samples for CE analysis were prepared by dissolving pure compounds in the buffer used for running electrolyte solution.

2.2. Post-column microchannel flow cell

The flow cell consists of two parts (Fig. 2a). One is a cylindrical rod-shaped (27 mm × 3 mm diameter) structure. Inside the structure, there is an "upside-down T" shaped channel formed by connection of the end part of the capillary column and the post-column microchannel. The column capillary extends from this assembled structure to the buffer reservoir where (+) high voltage is applied. The other is assembled with a square quartz tubing (20 mm × 10 mm square I.D.; Wale Apparatus, Hellertown, PA, USA) and two square stainless-steel plates. The bottom plate has an inlet for the buffer solution for flushing substances eluted from the microchannel. At the center of the cover plate, there is a 3-mm diameter hole into which the rod structure fits. The cover plate has two additional small holes; one is for the outlet of waste solution and the other is for the mount of a Pt electrode used to hold the cell at ground potential. The counter-gravity flow of the flushing buffer helps bubbles escape from the cell. The flow cell was constructed by putting all pieces together using various kinds of epoxy resins. Great care was taken of making the microchannel aligned vertically to a pair of opposite faces of the square quartz tubing.

Fig. 2b anatomically shows the cylindrical rod-shaped assembly that also consists of two parts. On the top of the lower part, the microchannel is formed along the cross-sectional axis of a borosilicate glass rod (10 mm × 3 mm diameter). The body of the channel is a piece of bisected fused-silica capillary. The procedure of making the channel is as follows. First, a groove of 0.4 mm width and 2 mm depth is made on the top surface of the rod using a diamond wafering blade. A 3-mm long fused-silica capillary (100 μm I.D. and 375 μm O.D.; Polymicro Technologies, Phoenix, AZ, USA) is placed in the groove and fixed with epoxy resin so that the

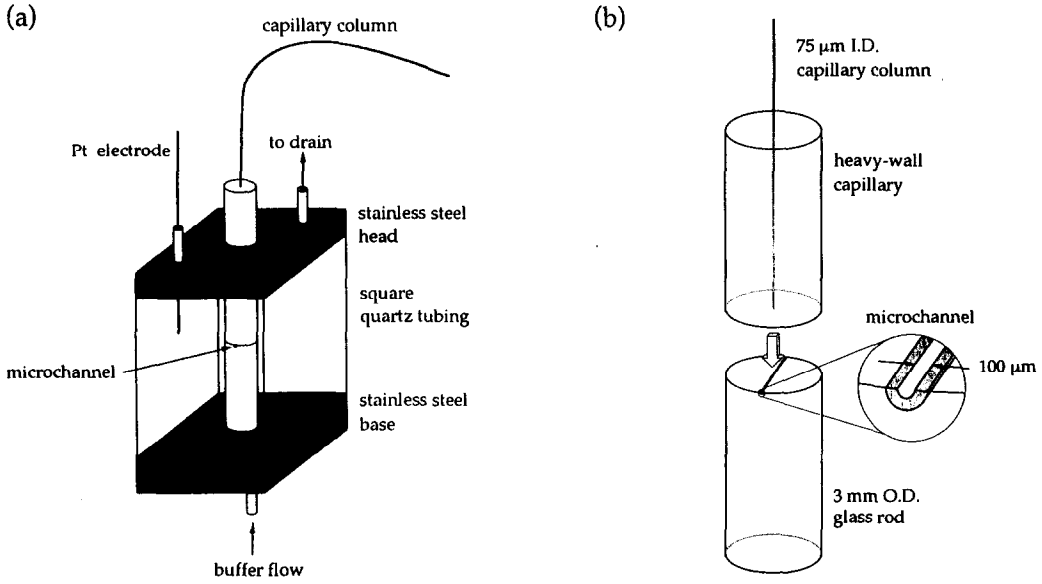

Fig. 2. (a) Whole construction of the post-column flow cell. (b) Anatomic view of the cylindrical rod-shaped assembly in the flow cell.

piece can be positioned vertically to the longitudinal axis of the rod. Finally, the top of the rod is finely ground until half of the cross section of the capillary is remained evenly along the length of the piece.

In the upper part of the cylindrical rod-shaped assembly, the end part of the capillary column (75 μm I.D. and 375 μm O.D.; Polymicro Technologies) is inserted through a piece of heavy-wall capillary (17 mm length, 0.4 mm I.D. and 3 mm O.D.; Wale Apparatus). The capillary column is fixed with epoxy resin and the bottom surface of the upper part is ground to form a fine and flat surface.

The construction of the assembly is completed by putting the two parts together using epoxy resin so that the cross-sectional center of the capillary column can sit on the middle of the longitudinal axis of the bisected capillary. Glass rod surfaces around the outlets of the microchannel are painted with an optically opaque epoxy (Epo-Tek 320; Epoxy Technology, Billerica, MA, USA), which ensures that the only light passing through the channel is detected by a light sensor.

2.3. CE apparatus with the post-column detection scheme

Fig. 3 represents a schematic of the homemade CE setup with the post-column UV–visible absorbance detector. A set of a deuterium (D_2) lamp and a monochromator built in the detector component (SP8480XR; Spectra-Physics, San Jose, CA, USA) of a commercial high-performance liquid chromatograph has been utilized as the light source of our CE system. A monochromatic light from the source is focused onto one end of the microchannel using a quartz plano-convex lens of 15.5 mm focal length. Temporal changes of the transmitted light intensity are transduced into corresponding voltage signals by a photomultiplier tube (PMT) module (HC120-01; Hamamatsu, Bridgewater, NJ, USA). The output signal from the PMT module is converted to the corresponding current signal via a 50-kΩ resistor. A current amplifier (428; Keithley, Cleveland, OH, USA) converts the current signal to an amplified voltage signal. The amplified output signal is then digitized by a 14-bit analog-to-digital (A/D) converter, and the

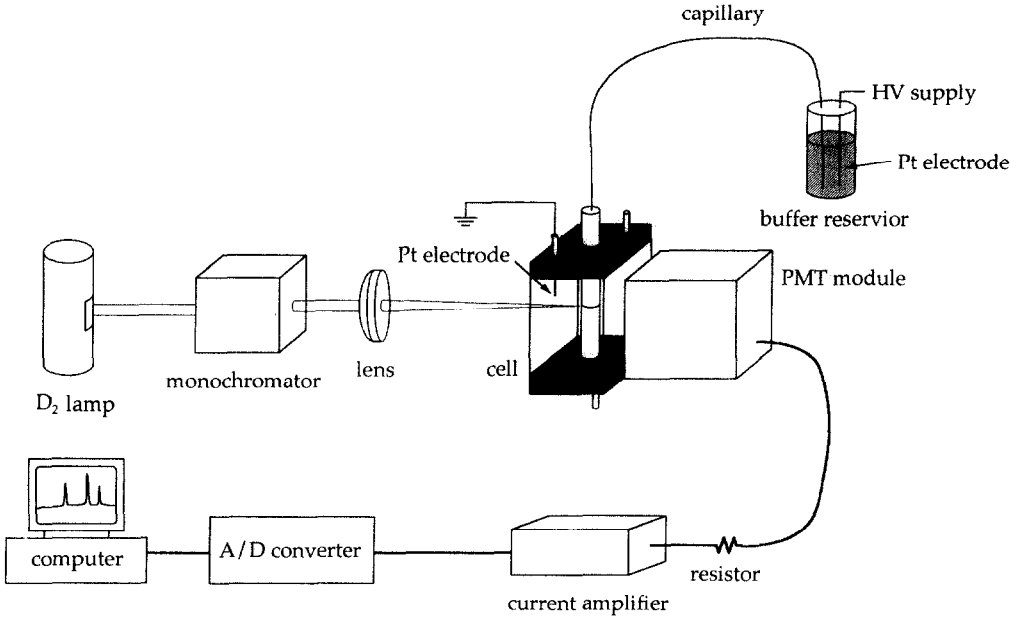

Fig. 3. CE setup with a UV–visible absorbance detector employing the post-column flow cell.

digitized signal is stored and processed using an IBM XT-compatible computer. Electropherograms are smoothed using the 7-point Savitzky-Golay algorithm before plotting them out.

A high-voltage power supply (EH60R1.5CT10; Glassman, Whitehouse Station, NJ, USA) is used to apply (+) high voltage across the fused-silica capillary column of 40 cm length. The buffer solution for auxiliary flows is fed into the flow cell by a HPLC pump (Spectroflow 4000; Kratos Analytical, Lancashire, UK).

2.4. CE apparatus with the on-column detection scheme

The CE setup built for the on-column UV absorbance detection is essentially the same as that for the post-column detection except for some differences. A neutral density (N.D.) filter of 1.0 N.D. (NDQ-100-1.00; CVI Laser, Albuquerque, NM, USA) is placed between the light source and the focusing lens. A 0.5-mm pinhole is used to confirm the dimension of the incident light on the detection window that is 40 cm from the injection end of the capillary column.

2.5. Capillary electrophoresis

The capillary columns were pretreated with 0.1 *M* sodium hydroxide solution, deionized water and running buffer solution in sequence. Each solution was pumped into the capillary for 3 min at a flow-rate of 15 μl/min using a syringe pump (Syringe Infusion Pump 22; Harvard Apparatus, South Natick, MA, USA). After each CE run, the column was rinsed with running buffer solution for 3 min.

Sample injection was accomplished manually by siphoning with a height of 20 cm for 10 s. To carry out CE separation, a high voltage was applied to the injection end of the capillary so that average electric field strength would be 300 V/cm. In the post-column detection method, auxiliary flow was maintained at a flow-rate of 0.7 ml/min after the high voltage was applied to the capillary for each CE run.

3. Results and discussion

According to Beer's law, the magnitude of absorbance for the same solution in absorbance detection is proportional to the optical path length of detection cell. In the case of the conventional on-column detection in CE, the effective path length of a parallel beam of light through a capillary of diameter d is equal to $\pi d/4$, which is due to the cylindrical cross section of capillaries [13]. However, the detection scheme using the post-column microchannel flow cell can utilize the full length of the microchannel as the optical path length.

Ideally, performance evaluation of the post-column microchannel flow cell should be carried out on commercial CE systems. Since no commercial CE instruments, however, were available to us, a simple homemade CE system was built for the evaluation. The system is easily interchangeable between on-column and post-column detection schemes without any changes in instrument except for the cells. Although the system has not performed as good as commercial ones, comparison of the post-column detection method with the on-column one gave us some qualitative information on the performance of the post-column flow cell.

Fig. 4 shows two electropherograms of FITC, which were obtained using the on-column and the post-column detection systems, respectively. The split peak top in Fig. 4b was attributed to superposition of noise signals on the FITC band. Since the I.D. of capillaries used was 75 μm and the length of the microchannel was 3 mm, the theoretical limit of sensitivity gain of the post-column detection over the on-column one would be 50. LODs (at S/N = 2) of FITC in the on-column and the post-column detection methods were $2.6 \cdot 10^{-6}$ *M* and $3.2 \cdot 10^{-7}$ *M*, respectively. Therefore, only an 8-fold enhancement of S/N was achieved by using the post-column microchannel flow cell.

As shown in the enlarged circle of Fig. 2b, the upper flat surface of the microchannel is a part of the bottom surface of the heavy-wall capillary. Because the refractive index of the heavy wall is greater than that of the buffer in the channel,

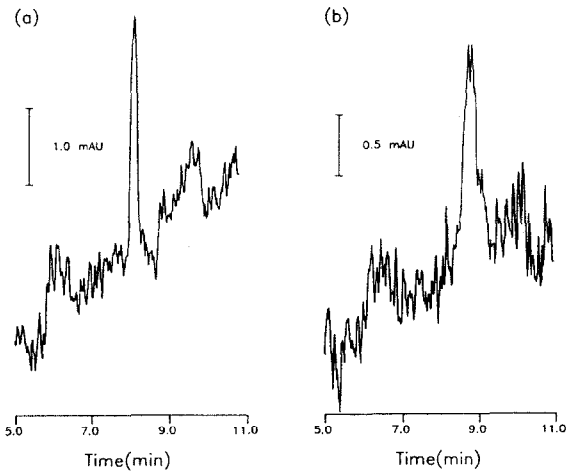

Fig. 4. Electropherograms of FITC. Capillary 75 μm I.D.; buffer, 10 mM phosphate (pH 6.9); sample injection, 10 s at 20 cm height difference; detection wavelength, 488 nm. (a) On-column detection system; sample concentration, $5.5 \cdot 10^{-6}$ M; separation column, 60 cm total length (40 cm to detector); applied voltage, 18 kV (300 V/cm). (b) Post-column detection system; sample concentration, $5.5 \cdot 10^{-7}$ M; separation column, 40 cm length; applied voltage, 12 kV (300 V/cm).

rays of light which are not parallel to the longitudinal axis of the channel can not experience any total internal reflections on the upper surface of the channel. Therefore if incident light is not collimated well, only a small portion of it can be transmitted through the channel. In consequence, probably, high background noise caused by the low light transmission through the microchannel resulted in the poor S/N gain obtained with the post-column design. Therefore a more intense light source and collimation of the light into a small-diameter beam are required to approach the theoretical limit of sensitivity of the post-column detection method. Because the post-column flow cells need collimated incident light to obtain greater sensitivities, coherent optical techniques, such as laser-induced fluorescence, would be better detection methods to which the cells can be applied.

The number of theoretical plates (N) was 10 000 for the on-column detection and 3500 for the post-column detection, which were obtained from the migration times and the full width at half maximum of peaks in both electropherograms of Fig. 4. Thus compared with the on-column detection, the post-column detection suffers 65% loss in efficiency, which corresponds to 44% loss in resolution ($R_S \approx N^{1/2}$). The detection volume of the post-column flow cell is very close to that of the 3-mm Z-cell with 75-μm I.D. Therefore if the influence of cell configuration on the electrophoretic process is similar to each other, it is expected that the maximum N and the loss in efficiency should not be very different in both cases. Much greater loss in efficiency with the post-column design, compared with the Z-shaped flow cells (less than 14% [12]), indicates that there must exist other sources of band broadening in the post-column microchannel flow cell. The auxiliary flows fed into the flow cell can cause some pressure effects which in turn can break the plug flow of electroosmosis. In addition to this, the T-connection between the capillary column and the microchannel may produce turbulence in flow, which could also cause band broadening.

The migration times of FITC in Fig. 4a and b are 8.2 min and 8.8 min, respectively. Although the length from the injection end of capillary columns to the detection window is the same (40 cm) in both cases, the longer migration time was obtained when the post-column microchannel flow cell was used. The difference in migration times may also be explained with the pressure effect mentioned above.

Linearity and reproducibility of the flow cell were evaluated with FITC electropherograms. Fig. 5 shows that linearity covers the range from $5.5 \cdot 10^{-7}$ M to $1.0 \cdot 10^{-5}$ M with the linear correlation coefficient r of 0.992. The flow cell provides a rather disappointing linear dynamic range, compared with linearity over 4.0 orders of magnitude for the ball lens-modified Z-shaped cells [12]. Since the detector compartment of our homemade CE system is not so light-tight as commercial ones, deviation from Beer's law could begin at lower concentrations. Although not shown in Fig. 5, the calibration curve begins to flatten at about $1 \cdot 10^{-5}$ M. However, any band broadening and tailing have not been observed up to about $1 \cdot 10^{-4}$ M, which indicates that the upper limit of the linearity of the post-

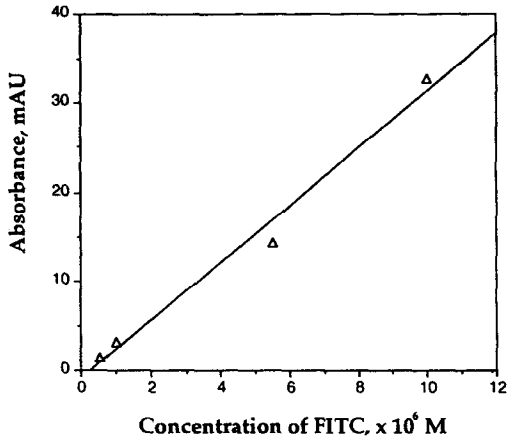

Fig. 5. Linear relationship between concentrations and peak heights of FITC for CE analysis using the post-column flow cell. Linearity covers sample concentrations from $5.5 \cdot 10^{-7}$ M to $1.0 \cdot 10^{-5}$ M and linear correlation coefficient r is 0.992.

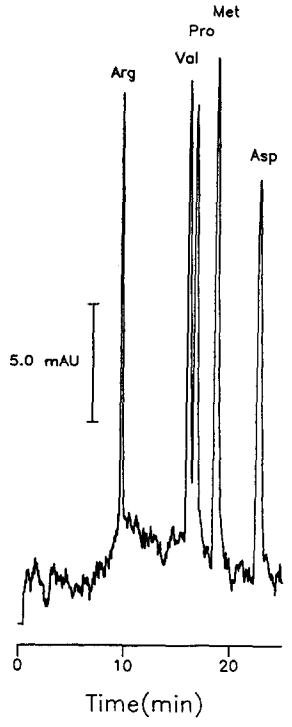

Fig. 6. Electropherogram of dansyl-amino acids obtained using the post-column flow cell. Capillary, 75 μm I.D., 58 cm length; buffer, 30 mM phosphate (pH 4.3); sample concentrations, $1.0 \cdot 10^{-5}$ M for each dansyl-amino acid; sample injection, 10 s at 20 cm height difference; detection wavelength, 216 nm; applied voltage, 17 kV (293 V/cm); Arg = dansyl-arginine; Val = dansyl-valine; Pro = dansyl-proline; Met = dansyl-methionine; Asp = dansyl-aspartic acid.

column flow cells is mainly attributed to stray light. The lower limit of the linearity is due to LOD that is limited by the high background noise caused by low light transmission. Reproducibilities in migration times and peak heights were 3.7% and 5.7%, respectively, in terms of relative standard deviation.

Fig. 6 demonstrates CE separation of a mixture of dansyl-amino acids using the setup equipped with the post-column flow cell. An equimolar mixture of five dansyl-amino acids was successfully separated by the system. LODs of dansyl-amino acids (216 nm) were the same as that of FITC (488 nm).

In the present design, the light incident to the post-column flow cell travels through a 1-cm thick buffer solution confined in a square quartz tubing (Fig. 2a). Although the same solution has been used for the running and the flushing buffers, in order to prevent attenuation of light intensity from scattering around the outlets of the microchannel, absorption by solvent and solute species (especially at short wavelengths) may cause low light transmission to some extent. Minimizing the distance between the flat optical windows and the outlets of the channel will be considered in future designs to improve performance of the cell. In this study for evaluating performance of the post-column flow cell as an absorbance detector cell, the contribution of absorption by buffer solutions to low light transmission would be negligible, because a visible wavelength of 488 nm has been mainly used. Also, to minimize the possibility of this contribution, phosphate buffers that are useful even below 215 nm, where the effect of background absorption is often significant [14], have been used throughout this study.

4. Conclusions

The post-column microchannel flow cell provides CE with an enhanced sensitivity for UV–visible absorbance detection. An 8-fold S/N improvement over on-column detection has been demonstrated, but it is far smaller than the expected 50-fold gain in sensitivity from the

extended optical path length. Optimizing light throughput, minimizing stray light and improving cell design are demanded to realize and expand practical usefulness of our post-column flow cell. It is expected that refined detection techniques employing the post-column microchannel flow cell will utilize all potential advantages of the cell, such as extended optical path length, easy optical coupling, easy modification to post-column derivatization/sensitive detection, and applicability to nearly all kinds of optical detection techniques for CE analysis.

Acknowledgements

The authors are grateful to the Korea Research Foundation and the Center for Biofunctional Molecules for the financial support of this work.

References

[1] J.W. Jorgenson and K.D. Lukacs, *Science*, 222 (1983) 266.
[2] M.J. Gordon, X. Huang, S.L. Pentoney, Jr. and R.N. Zare, *Science*, 242 (1988) 224.
[3] A.G. Ewing, R.A. Wallingford and T.M. Olefirowicz, *Anal. Chem.*, 61 (1989) 292A.
[4] H.H. Lauer and J.B. Ooms, *Anal. Chim. Acta*, 250 (1991) 45.
[5] D. Perrett and G. Ross, *Trends Anal. Chem.*, 11 (1992) 156.
[6] J.P. Landers, R.P. Oda, T.C. Spelsberg, J.A. Nolan and K.J. Ulfelder, *BioTechnology*, 14 (1993) 98.
[7] M. Albin, P.D. Grossman and S.E. Moring, *Anal. Chem.*, 65 (1993) 489A.
[8] S.E. Moring, J.C. Colburn, P.D. Grossman and H.H. Lauer, *LC·GC*, 8 (1990) 34.
[9] T. Tsuda, J.V. Sweedler and R.N. Zare, *Anal. Chem.*, 62 (1990) 2149.
[10] X. Xi and E.S. Yeung, *Appl. Spectrosc.*, 45 (1991) 1199.
[11] J.P. Chervet, R.E.J. van Soest and M. Ursem, *J. Chromatogr.*, 543 (1991) 439.
[12] S.E. Moring, R.T. Reel and R.E.J. van Soest, *Anal. Chem.*, 65 (1993) 3454.
[13] G.J.M. Bruin, G. Stegeman, A.C. van Asten, X. Xu, J.C. Kraak and H. Poppe, *J. Chromatogr.*, 559 (1991) 163.
[14] D.N. Heiger, *High Performance Capillary Electrophoresis—An Introduction*, Hewlett-Packard, Waldbronn, 1992, p. 95.